Available online at www.sciencedirect.com
SCIENCE DIRECT
International Journal of Heat and Mass Transfer 49 (2006) 3439–3447
International Journal of HEAT and MASS TRANSFER
www.elsevier.com/locate/ijhmt

The application of the CFD and Kriging method to an optimization of heat sink

Kyoungwoo Park *, Park-Kyoun Oh, Hyo-Jae Lim

Department of Mechanical Engineering, Hoseo University, 29-1 Sechul-ri, Baebang-myun, Asan, Chungnam 336-795, Republic of Korea

Received 11 July 2005; received in revised form 6 March 2006
Available online 11 May 2006

Abstract

The shape optimization of the plate-fin type heat sink with an air deflector is numerically performed to minimize the pressure loss subjected to the desired maximum temperature and geometrical constraints. A function evaluation using the FVM, in general, is required much computational costs in fluid/thermal systems. Thus, global approximate optimization techniques have been introduced into the optimization of fluid/thermal systems. In this study, the Kriging method, which is one of the metamodels, associated with the computational fluid dynamics (CFD) is used to obtain the optimal solutions. The Kriging method can dramatically reduce a computational cost by 1/6 times compared to that of the SQP method so that its efficiency can be validated. The results also show that when the temperature rise is less than 40 K, the optimal design variables are $B_1 = 2.44$ mm, $B_2 = 2.09$ mm, and $t = 7.58$ mm.

Keywords: Design optimization; Plate-fin type heat sink; CFD; Global approximate optimization; Kriging method

1. Introduction

Heat sinks have been generally used to control heat generated in electronic equipments effectively. It is true that an undesirable phenomenon such as increasing in the pressure loss commonly takes place in the plate-fin type heat sinks which fins are attached to the plate in order to enhance the heat transfer rate. Thus, high performance of heat sinks can be acquired through the design optimization which maximizes heat transfer and minimizes pressure drop.

Performance analysis and optimization of plate-fin type heat sinks have been performed for many years [1,2]. However, they have proposed the correlation equations for the design variables by considering only the flow and thermal characteristics of them.

In recent years, the use of commercial CFD codes for analyzing the flow and thermal fields in industrial applications has been dramatically increased due to their advanced computational capacity and analytic algorithm. In addition, many optimization techniques have been developed to obtain the optimal solutions. Therefore, much attention has been paid to the optimization of fluid/thermal systems by combining the CFD and optimization algorithm [3,4]. However, high computational cost for function evaluation and the occurrence of numerical noise are commonly confronted in fluid/thermal systems. Thus, a way to overcome the above-mentioned problems is to construct the approximated optimization techniques. These approximations are called ''metamodels'' which means a model of the model and it can effectively carry out the optimization of fluid/thermal systems.

A number of metamodeling techniques such as response surface models (RSM) [5], Kriging method [6], multivariate adaptive regression spline (MARS) [7], and radial basis function (RBF) [8] have been developed and applied to engineering applications. Among them, the Kriging method has been gaining attention recently because it offers the best linear unbiased estimator (BLUE). This method,

* Corresponding author. Tel.: +82 41 540 5804; fax: +82 41 540 5808.
E-mail address: kpark@office.hoseo.ac.kr (K. Park).

0017-9310/$ - see front matter © 2006 Elsevier Ltd. All rights reserved.
doi:10.1016/j.ijheatmasstransfer.2006.03.009

Nomenclature

B_1, B_2	base- and lower-part of fin width [m]
C_1, C_2, C_3	empirical constants in the k–ε model
d_k	distance between $\mathbf{x}_k^i$ and $\mathbf{x}_k^j$
$f(\mathbf{x})$	linear function of design variables x
$\hat{f}(\mathbf{x})$	Kriging estimation of $f(x)$
g_i	acceleration of gravity [m/s^2]
$g_j(\mathbf{x})$	inequality constraints
h	fin height [m]
h_v	length of air deflector [m]
H	height of heat sink ($=h+t$) [m]
k	turbulent kinetic energy [m^2 s^2]
k_s	thermal conductivity of solid [W/m K]
L	length of heat sink [m]
n_s	number of sampling points
n_{dv}	number of design variables
P	pressure [Pa]
ΔP	pressure drop [Pa]
Pr	Prandtl number
Q	dissipated heat [W]
$\mathbf{r}(\mathbf{x})$	correlation vector
$\mathbf{R}$	correlation matrix of Kriging
$R(\mathbf{x}^i, \mathbf{x}^j)$	correlation function between $\mathbf{x}_k^i$ and $\mathbf{x}_k^j$
t	basement thickness of heat sink [m]
T, T'	mean and fluctuating temperatures [K]
ΔT	temperature rise [K]
u_j, u_j'	mean and fluctuating velocities [m/s]
W	width of heat sink [m]
x, y, z	Cartesian coordinates [m]
$\mathbf{x}$	design variable vector
$y(\mathbf{x})$	objective function
$\hat{y}(\mathbf{x})$	least square estimator of $y(\mathbf{x})$
$z(\mathbf{x})$	departure of Kriging
$\boldsymbol{\beta}$	constant vector of Kriging
$\hat{\boldsymbol{\beta}}$	generalized least square estimator of $\boldsymbol{\beta}$
ε	dissipation rate of k [m^2/s^3]
μ, μ_t	viscosity and eddy viscosities [N s/m^2]
θ_j	thermal resistance [K/W]
$\boldsymbol{\theta} = (\theta_1, \ldots, \theta_{n_{dv}})$	correlation coefficients of Kriging
ρ	density [kg/m^3]
σ_k, σ_ε	turbulent Prandtl and Schmidt number for k and ε
σ^2	variance

one of the interpolation methods, does not create the estimated error and then is adequate to the model of computer experiments. Additionally, the Kriging method has a merit that an assumption of the order of the approximate function for optimization is not needed so that it is superior to general RSM.

In the present study, the optimal shape of plate-fin type heat sink with air deflector (or vortex generator) is obtained numerically by means of the Kriging method. In addition, in order to ensure the efficiency and reliability of the Kriging method for the optimal solutions, a comparison with sequential quadratic programming (SQP) method, which is one of local optimization strategies, is performed.

2. Kriging method

Kriging was conducted after Dr. D.G. Krige's work on the Rand gold deposit, in southern Africa [9]. Cressie [10] has introduced several Kriging techniques and he used them in predicting the value of a possible observation of a spatially distributed variable such as a mine grade, a soil characteristic, rain fall, gene frequency, or image sequence coding. Recently, the Kriging method was introduced for the design and analysis of computer experiments (DACE) by Sacks et al. [6]. This is used for fitting the model of the deterministic output to the realization of random processes for predicting efficiency and performed for the multidisciplinary design optimization (MDO) of the field of mechanics. Giunta [11] performed a preliminary investigation into the use of Kriging for the multidisciplinary design optimization of a high speed civil aircraft. Booker [12] used the Kriging to study the aero-elastic and dynamic response of a helicopter rotor. Recently, Ryu et al. [13] studied on the intake system to reduce the noise via the Kriging method. The Kriging method uses spatial correlation information and estimates the analysis results in the sampling points.

2.1. Mathematical model

Kriging is formulated as a combination of a linear regression model and departures, i.e.,

$$y(\mathbf{x}) = f(\mathbf{x}) + z(\mathbf{x}), \tag{1}$$

where $y(\mathbf{x})$ is the unknown function of interest of design variable $\mathbf{x}$, $f(\mathbf{x})$ a known linear function of $\mathbf{x}$, and $z(\mathbf{x})$ the realization of a stochastic with mean zero and variance σ^2, and nonzero covariance.

The covariance matrix of $z(\mathbf{x})$ is represented by

$$\mathrm{Cov}[z(\mathbf{x}^i), z(\mathbf{x}^j)] = \sigma^2 \mathbf{R}[R(\mathbf{x}^i, \mathbf{x}^j)], \quad i, j = 1, \ldots, n_s, \tag{2}$$

where $\mathbf{R}$ is a correlation matrix with diagonal of 1 (one) and $R(\cdot,\cdot)$ is the correlation function between any two points $\mathbf{x}^i$ and $\mathbf{x}^j$ of n_s sampled points. So, $R(\cdot,\cdot)$ reflects the association of the outputs generated by computer code and is specified by the users [14]. The following Gaussian correlation function is used to obtain it in this study,

$$R(\mathbf{x}^i, \mathbf{x}^j) = \prod_{k=1}^{n_{dv}} \exp\left[-\theta_k |\mathbf{x}_k^i - \mathbf{x}_k^j|^2\right]. \quad (3)$$

In Eq. (3), optimal correlation coefficients, $\boldsymbol{\theta} = (\theta_1, \ldots, \theta_{n_{dv}})$, on the design space $[0,1]^{n_s}$ is estimated by using a genetic algorithm.

Another term of interest is the correlation vector, $\mathbf{r}(\mathbf{x})$, between observed points $\mathbf{x}^1, \ldots, \mathbf{x}^{n_s}$ and an unobserved point $\mathbf{x}$. This can be expressed as follows:

$$\mathbf{r}(\mathbf{x}) = \mathbf{r}[R(\mathbf{x}, \mathbf{x}^i)] = \mathbf{r}[R(\mathbf{x}, \mathbf{x}^1), \ldots, R(\mathbf{x}, \mathbf{x}^{n_s})]. \quad (4)$$

2.2. Kriging estimator

Consider the following linear predictor of $y(\mathbf{x})$ at an untried $\mathbf{x}$:

$$\hat{y}(\mathbf{x}) = \mathbf{c}'(\mathbf{x})\mathbf{y}. \quad (5)$$

We can replace $\mathbf{y}$ by the corresponding random quantity of $Y = [Y(\mathbf{x}^1), \ldots, Y(\mathbf{x}^{n_s})]$, treat $\hat{y}(\mathbf{x})$ as random, and compute the mean squared error of this predictor averaged over the random process. The best linear unbiased estimator (BLUE) is obtained by choosing the $n_s \times 1$ vector, $\mathbf{c}(\mathbf{x})$, to minimize mean squared error,

$$\mathrm{MSE}[\hat{y}(\mathbf{x})] = E[\mathbf{c}'(\mathbf{x})\mathbf{y} - y(\mathbf{x})]^2. \quad (6)$$

That is,

$$\mathrm{MSE}[\hat{y}(\mathbf{x})] = (\mathbf{c}'(\mathbf{x})\mathbf{F}\boldsymbol{\beta} - \mathbf{f}'(\mathbf{x})\boldsymbol{\beta})^2 + \sigma^2[\mathbf{c}'(\mathbf{x}), -1]\begin{bmatrix}\mathbf{R} & \mathbf{r}(\mathbf{x}) \\ \mathbf{r}'(\mathbf{x}) & 1\end{bmatrix}\begin{bmatrix}\mathbf{c}(\mathbf{x}) \\ -1\end{bmatrix}. \quad (7)$$

For the unbiasedness constraint $\mathbf{F}\mathbf{c}'(\mathbf{x}) = \mathbf{f}(\mathbf{x})$ and $\mathbf{R}\mathbf{c}(\mathbf{x}) - \mathbf{r}(\mathbf{x}) - \mathbf{F}\lambda(\mathbf{x}) = 0$,

$$\begin{bmatrix}0 & \mathbf{F}' \\ \mathbf{F} & \mathbf{R}\end{bmatrix}\begin{bmatrix}-\lambda(\mathbf{x}) \\ \mathbf{c}(\mathbf{x})\end{bmatrix} = \begin{bmatrix}\mathbf{f}(\mathbf{x}) \\ \mathbf{r}(\mathbf{x})\end{bmatrix}. \quad (8)$$

So, Kriging estimates, $\hat{y}(\mathbf{x})$, of the response $y(\mathbf{x})$ at untried values of $\mathbf{x}$ are given by

$$\hat{y}(\mathbf{x}) = [-\lambda'(\mathbf{x}), \mathbf{c}(\mathbf{x})]\begin{bmatrix}0 \\ \mathbf{y}\end{bmatrix} = \mathbf{f}'(\mathbf{x})\tilde{\boldsymbol{\beta}} + \mathbf{r}'(\mathbf{x})\mathbf{R}^{-1}(\mathbf{y} - \mathbf{F}\tilde{\boldsymbol{\beta}}), \quad (9)$$

where $\hat{\boldsymbol{\beta}} = (\mathbf{F}'\mathbf{R}^{-1}\mathbf{F})^{-1}\mathbf{F}'\mathbf{R}^{-1}\mathbf{y}$ is the usual generalized least squared estimate of $\boldsymbol{\beta}$, $\mathbf{y}$ a column vector with responses of $\mathbf{x}^1, \ldots, \mathbf{x}^{n_s}$ and $\mathbf{f}$ a column vector of length n_s which is filled with ones. Assuming the Gaussian process, the likelihood is a function of the $\boldsymbol{\beta}$'s, variance σ^2 and correlation parameters. Given the correlation parameters, maximum likelihood estimator of σ^2 is defined as

$$\hat{\sigma}^2 = (\mathbf{y} - \mathbf{F}\tilde{\boldsymbol{\beta}})\mathbf{R}^{-1}(\mathbf{y} - \mathbf{F}\tilde{\boldsymbol{\beta}})/n_s. \quad (10)$$

With the definitions of $\tilde{\boldsymbol{\beta}}$ and $\hat{\sigma}^2$, the problem is to maximize the following equation:

$$\varphi(\boldsymbol{\theta}) = -(\det \mathbf{R})^{1/n_s}\hat{\sigma}^2, \quad (11)$$

which is a function of only the correlation parameter and the data. While any values for the $\boldsymbol{\theta} = (\theta_1, \ldots, \theta_{n_{dv}})$ in Gaussian correlation function create an interpolative approximation model, the best Kriging model is found by solving the unconstrained nonlinear optimization problem given by Eq. (11).

3. Optimization of heat sink

3.1. Physical specification of plate-fin type heat sink

The thermal system under consideration consists of duct, heat sink, and reactor and it is illustrated schematically in Fig. 1. Air induced by axial fan with constant temperature passes the duct and enters the channels formed by adjacent fins and heat sink basement. Finally, heated air, which absorbs the heat from the heat sink, flows out through exits located top wall of the reactor part.

The circulated figure in Fig. 1 depicts the detailed physical configuration of the plate-fins heat sink schematically because the objective of this study is to optimize the heat sink shape for the high performance of the fan-driven heat sink. The heat sink is made of aluminum and the fins are fabricated by extruding technique. The overall dimensions of heat sink are a length $L = 430$ mm, a width of $W = 188$ mm, and a height of $H = 65$ mm. Noting that the height of the heat sink (H) is sum of the fin height (h) and base thickness of heat sink (t). Two heat sources ($Q_1 = 348$ W, $Q_2 = 321$ W) with projected heating areas of dimensions of 62×122 mm, which are mounted on the top wall of heat sink, uniformly generate the heat by two different electric resistance heaters. A full-span vortex generator perpendicularly to the flow direction is mounted on the bottom wall of heat sink and it is located between two

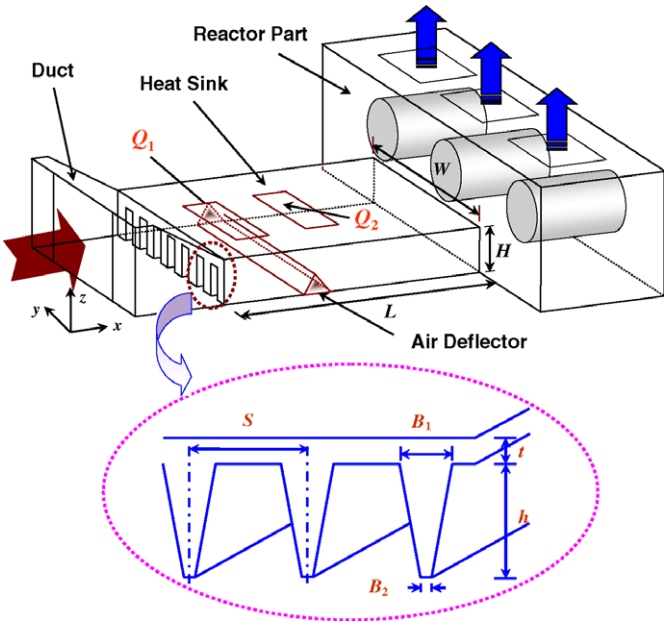

Fig. 1. Schematic configuration of the heat sink with air deflector.

heat sources. The air deflector has a triangular cross-section.

3.2. Mathematical formula for optimization

Optimization is to find the values of the design variables that minimize or maximize the objective function numerically while satisfying the constraints. Thus, optimization problems are made up of the following basic ingredients: design variable(s), objective function(s), constraint(s), and side constraint(s).

3.2.1. Objective function

For a given operating condition of a fan, increasing the heat transfer rate, however, is accompanied with increasing the pressure drop as a necessity. It is obvious that a high thermal performance (or cooling efficiency) can be obtained both by minimizing the thermal resistance and the pressure drop. Thus, the pressure drop (ΔP) and the thermal resistance ($\theta_j = \Delta T/Q = [T_{\max} - T_\infty]/Q$) have been generally adopted as the objective functions to be minimized in many industrial applications. Here ΔT is the temperature rise, $T_{\max}$ the junction (or maximum) temperature of heat sink, T_∞ the ambient temperature, and Q the heat generated. In a practical situation for a heat sink design, it is generally required that the maximum temperature (or temperature rise, ΔT) should be maintained under the desired one. Thus, the maximum temperature (or ΔT) is used as one of the constrained conditions and the pressure drop is adopted as an objective function only in this study.

3.2.2. Design variables

The geometric parameters which strongly influence the thermal performance of the heat sink are the base-part fin width (B_1), lower-part fin width (B_2), and base thickness of heat sink (t), as depicted in Fig. 1. Thus, three design variables are considered in this study: $x_1 = B_1$, $x_2 = B_2$, and $x_3 = t$ (i.e., $x = [B_1, B_2, t]$).

The nonlinear, constrained optimum design problem considered in this study can be expressed mathematically as follows:

Find

$$\mathbf{x} = \{B_1, B_2, t\}^{\mathrm{T}} \tag{12}$$

to minimize

$$y(\mathbf{x}) = \Delta P(= P_{\mathrm{in}} - P_{\mathrm{out}}) \tag{13}$$

subject to

$$g_1 = \frac{\Delta T}{(\Delta T_{\mathrm{specific}})} - 1 \leqslant 0, \quad g_2 = \frac{B_2}{B_1} - 1 \leqslant 0, \tag{14a}$$

$$1.25 \leqslant B_1 \leqslant 5.0\ \mathrm{mm}, \quad 1.25 \leqslant B_2 \leqslant 5.0\ \mathrm{mm},$$
$$7.0 \leqslant t \leqslant 25.0\ \mathrm{mm}, \tag{14b}$$

where $\mathbf{x}$ represents the design variable vector, $y(\mathbf{x})$ is the objective function which depends on $\mathbf{x}$, and $g_j(\mathbf{x})$ denotes the inequality constraints.

3.3. Flow and thermal fields

The physical problem considered in this study is the three-dimensional turbulent mixed convective flow and heat transfer of steady and incompressible fluid. The fluid properties are taken to be constant except for the density in the buoyancy terms of the momentum equation. The effects of viscous dissipation and radiation heat transfer are assumed to be negligibly small. Due to the symmetric geometry, the computation is only carried out one half of the physical domain. Using the above-mentioned assumptions, the following Reynolds-Averaged Navier–Stokes (RANS) equations based on the standard k–ε turbulent model [15,16] for mass, momentum, and energy are solved.

$$\frac{\partial(\rho u_j)}{\partial x_j} = 0, \tag{15}$$

$$\frac{\partial(\rho u_i u_j)}{\partial x_j} = -\frac{\partial P}{\partial x_i} + \frac{\partial}{\partial x_j}\left[\mu\left(\frac{\partial u_i}{\partial x_j} + \frac{\partial u_j}{\partial u_i}\right) - \overline{\rho u_i' u_j'}\right] + \rho g_i, \tag{16}$$

$$\frac{\partial(\rho u_j T)}{\partial x_j} = \frac{\partial}{\partial x_j}\left(\frac{\mu}{Pr}\frac{\partial T}{\partial x_j} - \overline{\rho u_i' T'}\right) + S_\phi, \tag{17a}$$

$$\frac{\partial}{\partial x_i}\left(k_{\mathrm{s}}\frac{\partial T}{\partial x_i}\right) + \dot{q} = 0, \tag{17b}$$

$$\frac{\partial(\rho u_j k)}{\partial x_j} = \frac{\partial}{\partial x_j}\left[\left(\mu + \frac{\mu_{\mathrm{t}}}{\sigma_k}\right)\frac{\partial k}{\partial x_i}\right] + G_k + G_b - \rho\varepsilon, \tag{18}$$

$$\frac{\partial(\rho u_j \varepsilon)}{\partial x_j} = \frac{\partial}{\partial x_j}\left[\left(\mu + \frac{\mu_{\mathrm{t}}}{\sigma_\varepsilon}\right)\frac{\partial \varepsilon}{\partial x_i}\right] + C_1\frac{\varepsilon}{k}(G_k + C_3 G_b) - C_2\rho\frac{\varepsilon^2}{k}. \tag{19}$$

We use the following boundary conditions to predict the flow and thermal fields in thermal system including the heat sink: the coolant of a constant temperature ($T_{\mathrm{in}} = 318$ K) induced by axial fan enters the system with a constant velocity ($u_{\mathrm{in}} = 1.27$ m/s) and a swirl condition of 60 rad/s. The corresponding turbulent kinetic energy and its dissipation rate are calculated from the following formula: $k_{\mathrm{in}} = 1.5 I_0^2 u_{\mathrm{in}}^2$, $\varepsilon_{\mathrm{in}} = k_{\mathrm{in}}^{3/2}/L_\varepsilon$, where the local turbulence intensity, I_0 is assumed to be 0.1 and L_ε is a length scale for dissipation, taken here as 80 mm (fan width). The pressure boundary condition is imposed at the outflow plane. For the other variables, the Neumann condition is employed. A no-slip boundary condition for all solid walls is assigned for velocity. For the turbulent kinetic energy and its dissipation rate, the wall function based on empirical wall law is employed. At the heat sink walls, the following thermal boundary conditions are imposed; two different heat fluxes are uniformly applied to the heat sink at the top wall of the heat sink by two heat sources. At the side wall and the top wall except for heat sources, the convective boundary condition is used ($h = 3$ W/m^2 K). At the bottom wall of heat sink, the adiabatic condition is adopted. The solid walls of the duct and reactor are assumed to be adiabatic. Symmetric conditions are imposed for all dependent variables at the plane of symmetry. The solutions are treated as converged ones when the sum of residual and the

relative deviation of dependent variables between consecutive iterations are less than 10^{-5}.

3.4. Numerical analysis

The governing equations for three-dimensional turbulent flow and thermal fields are solved using FLUENT which is a commercial finite volume CFD code [17]. The SIMPLE algorithm [18] is used to calculate the pressure correction equation in the momentum equation. The power law scheme is employed for the treatment of convection and diffusion terms. The number of cells for the computational domain has to be given sufficiently large (for baseline geometry, its number is around 1,300,000 cells) by considering the fine grid system at solid–gas interfaces.

4. Numerical methodology

In order to obtain the optimal values of the design variables for a plate-fin type heat sink by integrating the CFD and Kriging method, the sampling points are selected first and then the values of objective function, which are corresponded to them, are calculated by analyzing the flow and thermal fields of heat sink. The Kriging correlation coefficients are estimated using the sampling points and the response values. Finally, the optimal values can be achieved by adopting the completed model. In this study, the brief explanation for overall procedures is discussed below.

4.1. Selection of sampling points

For performing the optimization by Kriging method, some experimental points have to be selected by a design of experiments (DOE). In computer experiments, it is well known that the use of DOE, which is satisfied the concept of space filling, gives one confidence because it can be infiltrating the design space well. Therefore, Kriging method is more suitable than the classical ones such as a central composite design (CCD) [19] and Box–Behnken [20]. In this study, the DOE we used is Latin Hypercube design (LHD) [21], which is known as the effective sampling method in DACE.

Latin Hypercube design is the method that arrays the experimental points by generating a matrix with n_s rows and n_{dv} columns, where n_s is the number of levels being examined and n_{dv} is the number of design variables. The advantage of LHD appears when the output is dominated by only a few of the components of input variable like this study. This ensures that each of those components is represented in a fully stratified manner, no matter which components might turn out to be important.

4.2. Calculation of objective function

Once the sampling points are selected by the Latin hypercube design method, the objective function should be calculated by analyzing the flow and thermal fields of heat sink as discussed in Section 3.3.

4.3. Estimation of correlation coefficient

To solve the unconstrained nonlinear optimization problem in Eq. (11), we adapted the genetic algorithm [22] method, which is an adaptive heuristic search algorithm premised on the evolutionary ideas of natural selection and mutation. In many problems, it does not only provide an alternative method to solve the problem, but also consistently outperform other traditional methods in most of the problems link.

Fig. 2 presents a flow chart of genetic algorithm for estimating an optimal correlation coefficient in coefficients of Gaussian correlation function. To estimate an optimal correlation coefficient, data firstly has to be collected. Next, each initial chromosome is composed of a uniformly random number with length ($n_{dv} \times$ "the number of decimals"). This is substituted with a set of decimal number with length n_{dv}, which is the very candidate of $\boldsymbol{\theta} = (\theta_1, \ldots, \theta_{n_{dv}})$. Then, the distance between the two observed points $\mathbf{x}_i$ and $\mathbf{x}_j$ are calculated. Next, $\hat{\boldsymbol{\beta}}$ and $\hat{\sigma}$ can be calculated by using this correlation matrix, and the values of $\varphi(\boldsymbol{\theta})$ in Eq. (11) are evaluated and compared with each other. In the last stage, selection, crossover and mutation process in genetic algorithms are applied to generate the new chromosomes. The optimal correlation coefficient $\boldsymbol{\theta} = (\theta_1, \ldots, \theta_{n_{dv}})$ is

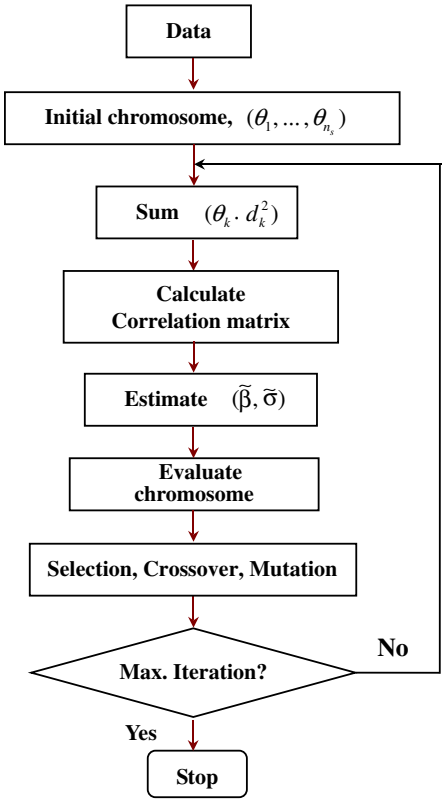

Fig. 2. Procedure for obtaining the Kriging correlation coefficients.

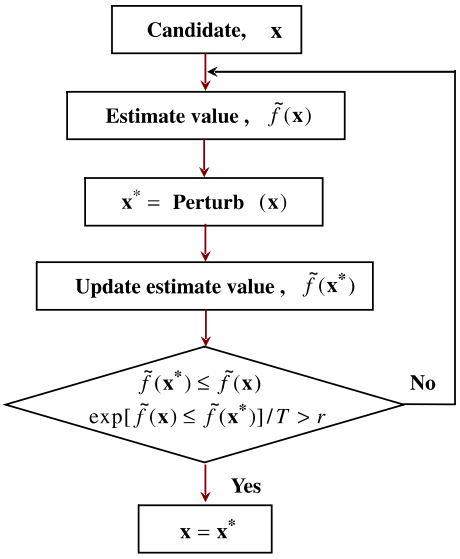

Fig. 3. Procedure for obtaining the optimal level of Kriging.

updated continuously until the iteration number is reached at its maximum one (i.e., 100,000).

4.4. Approximate optimization

Simulated annealing (SA) [23] is a technique for combinatorial optimization problems, such as for optimizing of very many variables. The concept is based on liquid freezing or metal crystallizing in the process of annealing. In the cooling process, the system becomes more ordered and approaches a frozen ground state, that is, lowest energy state. If the initial temperature of the system is too low or cooling is done insufficiently slowly the system may become quenched forming defects or freezing out in meta-stable states. That is, SA is a technique to find a best solution with a slower cooling schedule and probabilistic computational process.

Fig. 3 shows a procedure of simulated annealing to find an optimal level in design space by using Kriging estimate. After the optimal correlation coefficient, $\boldsymbol{\theta} = (\theta_1, \ldots, \theta_{n_{dv}})$, is determined with the genetic algorithm in Section 4.3, Kriging estimate values of all points in design space can be calculated by Eq. (9). Now, a point $\mathbf{x}$ in design space is selected and its Kriging estimate value is calculated. Then, $\mathbf{x}^*$ is selected by perturbing $\mathbf{x}$ and its Kriging estimate value is calculated. In the last stage, of the two points, one point remains on the annealing schedule. When a terminate condition is satisfied, this process is completed with an optimal level.

5. Results and discussion

The optimal values of the design variables in plate-fin type heat sink are numerically acquired by using the CFD and Kriging method. At first, the sampling points are calculated by considering the upper/lower limits of design variables and they are used for optimization.

5.1. Effect of air deflector

In order to investigate the effect of air deflector on the flow and thermal characteristics of heat sink before the optimization is carried out, we compare them for the cases of with and without air deflector and the results calculated are listed in Table 1. Table 1 presents the maximum temperature (T_j), temperature rise ($\Delta T = T_j - T_\infty$) and pressure drop ($\Delta P$) for two cases. In the table, all operating conditions and geometric configurations are same as the baseline geometry. Air deflector has a triangular cross-section of 20 mm and a width of 188 mm, as shown in Fig. 1. As can be seen in Table 1, for the case of with air deflector, the maximum temperature is predicted as 362.3 K and is reduced by 4.2 K compared to that of without air deflector, while the pressure drop is increased from 38.15 Pa to 41.29 Pa. These phenomena can be simply explained by the following two facts; the breaking the thermal boundary layer and the increasing the flow resistance, respectively, by the existence of air deflector. From the flow and thermal analyses of system, it can be found that *maximum temperature* is occurred at the rear-heat source (i.e., $Q_2 = 321$ W). From now on, all results obtained are those of with air deflector. Table 1 also illustrates that the temperature rise of 44.31 K is exceeded the general desired temperature rise of 40 K which is corresponding to the maximum temperature for safe operating of thermal system. This means that the plate-fin type heat sink must be optimized for the thermal stability.

5.2. Optimal solutions

Table 2 shows the sampling points selected by using the LHD method. In this case, they are selected according to the upper and lower limits of the design variables, which is defined in Eq. (14b). In this study, the number of sampling points are determined as 30 (that is, $10 \cdot n_{dv}$) by considering the accuracy and efficiency of the metamodel. In order to optimize the shape of heat sink, the pressure drop and maximum temperature in the heat sink should be predicted for each selected sampling point and their values are listed at columns of 5 and 6 in Table 2. Because the optimization problem considering this study is minimized the pressure drop while the maximum temperature is satisfied within the desired one, the correlation coefficients are calculated using the pressure drop and maximum temperature in Table 2 and then the optimal solutions are estimated by

Table 1
Maximum temperature (T_j) and pressure drop (ΔP) for the cases of with and without air deflector

	w/o air deflector	w/ air deflector
Maximum temperature, T_j (K)	366.48	362.31
Temperature rise, ΔT (K)	48.48	44.31
Pressure drop, ΔP (Pa)	38.15	41.29

Table 2
Sampling points and corresponding to values of performance functions

No.	x_1	x_2	x_3	ΔP	T_{max}
1	3.8708	5.0042	8.7333	153.114	352.644
2	2.7375	4.7208	10.6	95.886	354.431
3	3.7292	2.1708	9.5333	77.886	355.088
4	3.1625	3.1625	14.0667	96.015	354.792
5	4.2958	2.4542	14.8667	135.821	353.879
6	2.0292	1.4625	8.2	39.376	359.663
7	1.6042	3.8708	7.1333	49.263	358.439
8	1.7458	2.8792	8.4667	45.474	358.562
9	1.8875	3.3042	11.1333	56.801	357.147
10	1.4625	1.3208	10.8667	38.071	360.702
11	2.4542	4.8625	7.9333	81.395	355.311
12	4.7208	3.0208	9.0	134.122	352.999
13	4.8625	1.6042	10.3333	110.843	354.079
14	5.2875	4.0125	9.8	238.381	351.473
15	5.4292	3.4458	13.2667	262.828	351.819
16	3.0208	2.7375	7.4	62.150	356.144
17	2.1708	4.4375	14.3333	87.141	355.406
18	4.1542	5.1458	13.5333	218.612	351.982
19	4.4375	1.7458	13.0	112.419	354.332
20	2.5958	2.5958	10.0667	59.462	356.531
21	2.3125	2.0292	12.4667	56.498	357.402
22	4.5792	5.2875	11.4	266.645	351.377
23	5.0042	1.8875	7.6667	109.035	354.027
24	3.3042	3.7292	9.2666	90.089	354.328
25	3.4458	2.3125	11.6667	80.562	355.188
26	3.5875	3.5875	11.9333	109.345	353.803
27	1.3208	4.2958	12.7333	60.872	357.451
28	2.8792	5.4292	12.2	127.800	353.728
29	4.0125	4.1542	14.6	167.697	352.857
30	5.1458	4.5792	13.8	322.814	351.347

the Kriging method. Therefore, the optimal values of the heat sink strongly depend on the values of ΔP and T_{max}.

To explain the typical results for optimization, the initial and optimized designs for the temperature rise of 40 K are listed in Table 3. When minimizing the pressure drop in the heat sink, it is important to restrict the temperature rise which is the most important operating factor for the thermal stability of heat sink. As shown in Table 3, the optimized thermal resistance of 0.059 K/W represents a reduction of 10.6% compared to the initial thermal resistance of 0.066 K/W due to the decrease of temperature rise (4.3 K). However, the optimized pressure drop is increased by 10.3% from 41.29 Pa to 45.54 Pa. It can be also seen from Table 3 that the optimal values of all design variables are increased compared to those of the initial variables.

Table 3
Initial and optimized designs for $\Delta T < 40$ K

	Initial	Optimal
B_1 (mm)	2.0	2.44
B_2 (mm)	1.5	2.09
t (mm)	7.0	7.58
Thermal resistance, θ_{ja} (K/W)	0.066	0.059
Pressure drop, ΔP (Pa)	41.29	45.54
Max. temperature, T_{max} (K)	362.31	357.99
Temperature rise, ΔT (K)	44.31	39.99

Especially, B_1 and B_2 are thickened by 22% and 39.3%, respectively, compared to the initial value and it is obvious that they are the most important variables to enhance the thermal performance of heat sink. This is due to the fact that the velocity in flow passage formed by adjacent fins should increase to reduce the temperature rise (that is, enhance the heat transfer rate) and it results in the increase of pressure drop.

Table 4 shows the correlation coefficient ($\boldsymbol{\theta}$) which can be obtained by maximizing the likelihood function ($\varphi(\boldsymbol{\theta})$), the optimal values ($\mathbf{x}_{opt}$), and objective function (ΔP_{min}) according to the desired maximum temperature (T_{max}). The correlation coefficient of $\boldsymbol{\theta} = (\theta_1, \ldots, \theta_{n_{dv}})$ is corresponding to the design variables of B_1, B_2 and t. It can be seen in Table 4 that different optimal values are obtained according to the desired maximum temperature and they cause to change the objective functions (ΔP_{min}). If the value of required maximum temperature is small ($T_{max} = 355$ K), the larger values of the design variables are acquired compared to that of large T_{max} and they are also plotted in Fig. 4 in order to explain variations of the optimal design variables for five different temperature rises. These phenomena result from the following reasons; for a fixed volume of heat sink ($L \times W \times H =$ constant), increasing the design variables retards the development of the thermal boundary layer. It results in the thinner thermal boundary layer and the larger friction loss due to the increased velocity. Thus, the maximum temperature is reduced and the pressure drop is increased as the design variables are thickened as shown in Table 4.

A set of optimal solutions for the objective function can be constructed so that the designer can select the preferred solution based on Table 4. For this purpose, the relationship between the pressure drop (Δp) and the temperature

Table 4
Correlation coefficients ($\boldsymbol{\theta} = \theta_1, \theta_2, \theta_3$) and optimal solutions for various maximum temperatures

T_{max} [K]	$\boldsymbol{\theta}$		Optimal	
	ΔP	T_{max}	$\mathbf{x}_{opt}$	ΔP
355	[2.402, 1.111, 0.101]	[1.280, 0.088, 0.141]	[3.462, 2.852, 8.489]	76.86
356	[2.468, 1.085, 0.103]	[1.361, 0.213, 0.168]	[3.110, 2.498, 8.298]	62.07
357	[1.996, 1.023, 0.077]	[1.013, 0.102, 0.120]	[2.766, 2.260, 7.955]	53.05
358	[2.168, 0.963, 0.074]	[1.145, 0.145, 0.137]	[2.443, 2.091, 7.582]	45.54
359	[1.789, 0.893, 0.061]	[1.028, 0.150, 0.122]	[2.174, 1.935, 7.117]	40.23

$\mathbf{x}_{opt} = [B_1, B_2, t]_{opt}$.

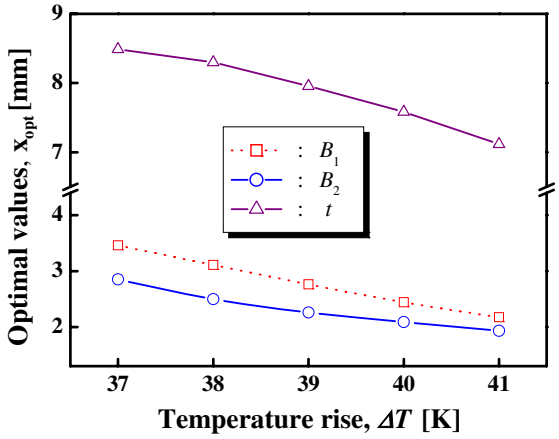

Fig. 4. Variations of optimal design variables for maximum temperature.

rise (ΔT) is illustrated in Fig. 5. The points on the curve from (a) to (e) are one of the optimal solutions. The results can be very helpful to designers in order to achieve the optimization of the heat sink. For example, when designers want to focus on decreasing the thermal resistance rather than decreasing the pressure drop, they can select the points such as (a) or (b) on the curve of Fig. 5 and then read the corresponding optimal design variables in Table 4. For the thermal management of the heat sink, it is important to remark that the most important goal is to maximize the heat transfer rate or minimize the thermal resistance and this is easily achieved by the increase of the velocity between fins and the heat transfer area. However, the minimized pressure drop is strongly related to the specific cost, because the pressure drop determines the size of the fan needed to blow the cool air through the channel. Therefore, choosing one of the optimal solutions in Fig. 5 is dependent on the heat sink designers.

Main difficulty faced by numerical analysis of fluid flow and heat transfer using the finite volume method (FVM) is caused by the requirement of much computational cost. Thus, for the optimization of fluid/thermal systems, enhancement of the efficiency which can reduce the overall

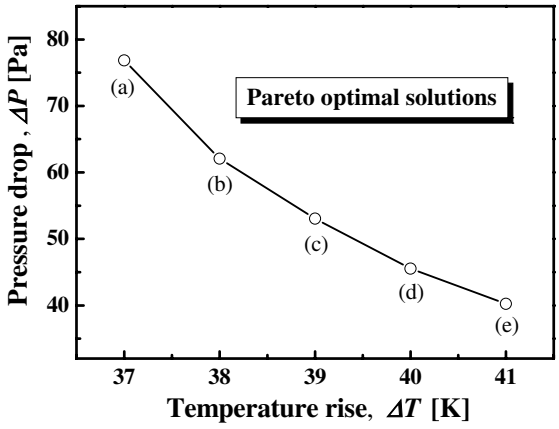

Fig. 5. Temperature rise vs. pressure drop.

CPU time for optimization process becomes very important issue which has to be resolved rather than improvement of the accuracy of optimal solutions. In the present study, in order to investigate the accuracy and efficiency of the Kriging method, we compare the objective function and NFC with those of SQP method for the same geometric configuration, which is reported in Ref. [24]. The "NFC" is the "Number of function calls" and it implies the total number of flow and thermal analyses required (or total number of changes of design variables proposed by optimizer) throughout the optimization process. Table 5 shows that the objective function for the Kriging method has lower values than that for the SQP method for all temperature rises. For the NFC, overall computational time for optimization of the Kriging method is just 16% of SQP method (that is, total NFC for the Kriging and SQP methods are 30 and 180, respectively). From these two facts, it is clear that the Kriging method is superior to the SQP method within the range of this study.

Actually, the optimal values and their corresponding objective function which can be obtained by the Kriging method must be estimated ones. Therefore, the values of objective function ($\Delta P_{\min}$) should be checked in order to validate the Kriging method. For this, the estimated and calculated values of objective function according to the optimal design variables are presented in Table 6. The meaning of "calculated" is values obtained by analyzing the flow and thermal fields in the heat sink by the computational fluid dynamics. Table 6 shows that the estimated values $\Delta P_{\min}$ are very good agreement with those of calculated. That is, for $\Delta T < 37$ K , the estimated value by the Kriging method and calculated one by CFD are 76.86 Pa

Table 5
Accuracy and efficiency of Kriging method compared to SQP method

ΔT[a]	ΔP [Pa]		NFC[b]	
	Kriging	SQP [24]	Kriging	SQP [24]
37	76.86	N/A	30	N/A
38	62.07	62.11		67
39	53.05	53.36		51
40	45.54	46.72		42
41	40.23	41.94		21
Total			30	181

[a] $\Delta T = T_{\max} - T_{\infty} = (T_{\max} - 318)$ K.
[b] NFC: number of function calls.

Table 6
Validation of optimal results for Kriging method

ΔT	$\mathbf{x}_{opt}$	ΔP [Pa]	
		Kriging	CFD
37	(3.462, 2.852, 8.489)	76.86	76.94
38	(3.110, 2.498, 8.298)	62.07	62.43
39	(2.766, 2.260, 7.955)	53.05	53.94
40	(2.443, 2.091, 7.582)	45.54	46.79
41	(2.174, 1.935, 7.117)	40.23	41.81

$\mathbf{x}_{opt} = [B_1, B_2, t]_{opt}$.

and 76.94 Pa, respectively, and the difference is just 0.1%, while $\Delta T < 41$ K is 3.8%. It can also be seen in Table 6 that the difference between estimated and calculated values is reduced as the temperature rise is decreased. From the results of Tables 5 and 6, it can be easily concluded that the Kriging method, which is one of the global approximate optimization techniques, can optimize the heat sink efficiently and accurately.

6. Conclusions

We numerically obtained the optimum design variables of a plate-fins heat sink to minimize the pressure drop while the desired maximum temperature is satisfied. The thermal and flow characteristics were analyzed using the finite volume method. The Kriging method, which is one of metamodels, was used for completing the optimization. As the results of optimization, the following conclusions were obtained: the most dominant design variables for the pressure drop and thermal resistance were the base-part fin width (B_1), and the lower-part fin width (B_2), while the effect of base thickness (t) on them was relatively small compared to the other two design variables. The results also showed that the optimal design variables for the temperature rise of 40 K were $B_1 = 2.44$ mm, $B_2 = 2.09$ mm, and $t = 7.58$ mm. In this case, the thermal resistance for the optimum model was decreased by 10.6%, while the pressure drop was increased by 10.3% compared to those of the initial model. It was also found that the Kriging method can be a popular technique by comparing with a local optimization technique for its accuracy and efficiency. The results of this work can offer designers the information they need to select the optimal design variables corresponding to the preferred objective functions.

Acknowledgement

This work was supported by Grant No. RTI04-01-02 from the Regional Technology Innovation Program of the Ministry of Commerce, Industry and Energy (MOCIE).

References

[1] G. Ledezma, A. Bejan, Heat sink with sloped plate fins in natural and forced convection, Int. J. Heat Mass Transfer 39 (1996) 1773–1783.
[2] S.W. Chang, L.M. Su, T.L. Yang, S.F. Chiou, Enhanced heat transfer of forced convective fin flow with transverse ribs, Int. J. Therm. Sci. 43 (2004) 185–200.
[3] K. Park, D.H. Choi, K.S. Lee, Optimum design of plate heat exchanger with staggered pin arrays, Numer. Heat Transfer, Part A 45 (2004) 347–361.
[4] K. Park, D.H. Choi, K.S. Lee, Numerical shape optimization for high performance of a heat sink with pin-fins, Numer. Heat Transfer, Part A 46 (2004) 909–927.
[5] G.E.P. Box, W.G. Hunter, J.S. Hunter, Statistics for Experimenters, John Wiley & Sons, NY, 1978.
[6] J. Sacks, W.J. Welch, T.J. Mitchell, H.P. Wynn, Design and analysis of computer experiments, Statist. Sci. 4 (1989) 409–435.
[7] J.H. Friedman, Multivariate adaptive regression splines, The Ann. Statist. 19 (1991) 1–141.
[8] R.L. Hardy, Multi-quadratic equations of topography and other irregular surfaces, J. Geophys. Res. 76 (1971) 1905–1915.
[9] D.G. Krige, A statistical approach to some basic mine valuation problems on the Witwatersrand, J. Chem. Metallurgical Mining Soc. South Africa 52 (1951) 119–139.
[10] N.A.C. Cressie, Statistics for Spatial Data, John Wiley & Dons, New York, 1993.
[11] A.A. Giunta, Aircraft multidisciplinary design optimization using design of experiments theory and response surface model, Ph.D. thesis and MAD Center Report No. 97-05-01, Department of Aerospace and Ocean Engineering, Virginia, Polytechnic Institute and State University, Blacksburg, VA, 1997.
[12] A.J. Booker, Cases studies in design and analysis of computer experiments, Proc. of the Section on Physics and Engineering Sciences, 1996.
[13] J.S. Ryu, M.S. Kim, K.J. Cha, T.H. Lee, D.H. Choi, Kriging interpolation method in geostatistics and DACE model, KSME Int. J. 16 (5) (2002) 619–632.
[14] T.W. Simpson, A concept exploration method for product family design, Ph.D. thesis, Department of Mechanical Engineering, Georgia Institute of Technology,1998.
[15] W. Rodi, Turbulence models and their applications in hydraulics—a state art of review, Book Publication of International Association for Hydraulic Research, Delft, Netherlands, 1984.
[16] K. Abe, T. Kondoh, Y. Nagano, A two-equation heat transfer model reflecting second-moment closures for wall and free turbulent flows, Int. J. Heat Fluid Flow 17 (1996) 228–237.
[17] FLUENT 6 User's Guide, FLUENT Inc., Lebanon, New Hampshire, 2003.
[18] S.V. Patankar, Numerical Heat Transfer and Fluid Flow, Hemisphere, Washington, 1980.
[19] G.E.P. Box, K.B. Wilson, On the experimental attainment of optimum conditions, J. Roy. Statist. Soc., Ser. B 13 (1951) 1–45.
[20] G.E.P. Box, D.W. Behnken, Some new three level designs for the study of quantitative variables, Technometrics 2 (1960) 455–475.
[21] M.D. McKay, R.J. Beckman, W.J. Conover, A comparison of three methods for selecting values of input variables in the analysis of output from a computer code, Technometrics 21 (1979) 239–245.
[22] J.H. Holland, Adaptation in Natural and Artificial Systems, University of Michigan Press, 1975.
[23] S. Kirkpatrick, C.D. Gelatt Jr., M.P. Vecchi, Optimization by simulated annealing, Science 220 (1983) 671–680.
[24] K. Park, D.H. Choi, Shape optimization of a plate-fin type heat sink with triangular-shaped vortex generator, KSME Int. J. 18 (2004) 1590–1603.